



High temperature initiation and propagation of cracks in 12%Cr-steel turbine disks

S. Foletti, A. Lo Conte, S. Salgarollo, F. Bassi

Department of Mechanical Engineering, Politecnico di Milano, Milano (Italy)

stefano.foletti@polimi.it, antonietta.loconte@polimi.it, stefano.salgarollo@mail.polimi.it, federico.bassi@mail.polimi.it

A. Riva

AEN, Genova, (Italy)

andrea.riva@aen.ansaldo.it

ABSTRACT. This work aims to study the crack propagation in 12%Cr steel for turbine disks. Creep Crack Growth (CCG) tests on CT specimens have been performed to define the proper fracture mechanics which describes the initiation of the crack propagation and the crack growth behaviour for the material at high temperature. Results have been used to study the occurrence of crack initiation on a turbine disk at the extreme working temperature and stress level experienced during service, and validate the use of C^* integral in correlating creep growth rate on the disk component, in case C^* is numerically calculated through FEM analysis or calculated by the use of reference stress concept.

SOMMARIO. In questo lavoro si studia la propagazione di cricche in regime di scorrimento viscoso su una lega 12%Cr tipicamente impiegata per la realizzazione di dischi turbina. Sono state condotte prove di CCG al fine di ricavare i parametri che caratterizzano l'inizio della propagazione della cricca per scorrimento viscoso e di valutare quale parametro della meccanica della frattura correla la velocità di accrescimento della cricca. I risultati sono stati applicati: 1) allo studio dell'inizio di propagazione di un difetto per scorrimento viscoso su un disco turbina; 2) alla validazione dell'impiego del parametro C^* della meccanica della frattura per correlare l'accrescimento della cricca sul disco turbina, sia quando il parametro C^* è valutato numericamente con analisi ad elementi finiti, sia quando il suo calcolo è basato sul concetto di sforzo di riferimento.

KEYWORDS. Fracture mechanics; Creep Crack Growth; 12Cr steel; C-integral; Reference stress.

INTRODUCTION

For design and safety assessment purposes it is often necessary to establish the significance of defects in components subjected to creep and creep-fatigue loading. The behaviour of a defect in a component operating at high temperature may be described as a sequence of three stages. The first stage is an incubation period where the creep damage builds up in front of the crack tip, but any significant crack growth occurs. The second stage is a steady state crack process, where the crack propagates through the material with cracking speed nearly constant. The third one is creep rupture due to accumulation of creep damage in the cracked ligament. A number of assessment procedures are available for dealing with this situation. These include British Energy R5 [1], BS 7910 [2] codes, and more recently the

European FITNET procedure [3]. Each of these procedures uses a combination of continuum mechanics and fracture mechanics concepts to make a creep loading assessment. The information required for the assessment is:

- the operating conditions;
- the geometry of the defect;
- material data;
- structural analysis in order to transfer material data to the behaviour of complex structures.

When such procedures are used at the design stage, the size of postulated defects is determined by the use of non-destructive inspection methods. Otherwise, the information may be used to assess whether a defect of a given size will grow to an unacceptable size under a given exposure time to high temperature.

For the evaluation of the crack initiation the use of Two Criteria Diagram (2CD) promised to be the appropriate way to treat the problem of different types of damage behaviour in components [4]. Inside the no damage zone of Fig. 1 highlighted in green, cracks do not initiate and propagate while inside the damage zone highlighted in red, crack initiation and propagation is possible. In the 2CD [5] for creep crack initiation the nominal stress $\sigma_{n,pl}$ considers the stress situation in the ligament while the ideal elastic stress intensity factor K_{Iid} , describes the condition at the crack tip, at a time zero. The loading parameters ($\sigma_{n,pl}$, K_{Iid}) are normalized by the respective time and temperature dependent data, which indicate the strength of the material against crack initiation. The normalized parameters are, for the stress in the ligament, the stress ratio:

$$R_{\sigma} = \sigma_{n,pl} / \sigma_R \quad (1)$$

and, for the crack tip, the stress intensity ratio

$$R_K = K_{Iid} / K_{Ii} \quad (2)$$

The value σ_R is the creep rupture strength of the material while the parameter K_{Ii} characterizes the creep crack initiation of the material. These parameters shall be determined from creep rupture tests on cylindrical specimens and from Creep Crack Growth (CCG) tests on CT specimens respectively. While R_k considers the presence of a defect in the component, R_{σ} just take into account the creep effects on smooth specimens away from possible defects. The 2CD defines three mechanisms of damage responsible for crack initiation. A low value of the ratio $K_{Iid} / \sigma_{n,pl}$ indicates the beginning of the propagation due to the widespread damage in the resistant section behind the crack tip, a high ratio $K_{Iid} / \sigma_{n,pl}$ indicates the initiation of the propagation due to localized damage of the crack tip, while between these extremes a transition zone indicates initiation due to a mixed damage mode. The two criteria method described has been developed as a way of practice to transfer creep crack initiation data, from specimens with different size to larger components with similar characteristics and crack tip situation, and its applicability has been well proved [6].

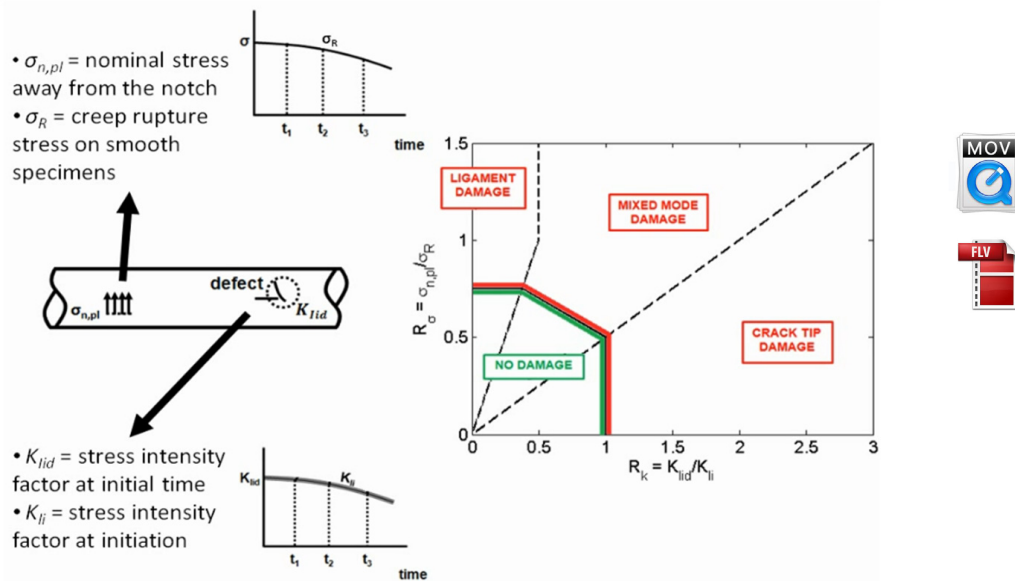


Figure 1: Prediction of creep crack initiation time by using 2CD.



The theory behind the correlation of high temperature crack growth data essentially follows that of elastic-plastic fracture mechanics. The parameter to describe the creep crack growth behaviour has been discussed for a number of years [7, 8] and it is well known that for situations where linear elastic conditions prevail (short times and/or low loads) the linear elastic stress intensity factor, K , may be used to predict creep crack growth. For creep-ductile materials under steady state creep conditions however, the linear elasticity may no longer be applicable and the stress intensity factor do not properly characterize crack growth rates. This is demonstrated by considering influences of the load level and temperature. The crack tip stress and strain rate fields of ductile materials under steady crack growth are characterised by the parameter C^* which can successfully correlate creep crack growth. The C^* parameter is defined as the stabilized value of the parameter $C(t)$ for $t \rightarrow \infty$, i.e. when the effect of creep caused the complete redistribution of stresses behind the crack tip:

$$C^* = C(t \rightarrow \infty) = \int_{\Gamma} \dot{W}(t) dy - T_i \frac{\partial \dot{u}_i}{\partial x} ds \quad (3)$$

where Γ is a contour around the crack tip, $\dot{W}(t)$ the strain energy density rate, T_i the components of the traction vector and \dot{u}_i the components of the displacement rate vector. By analogy between steady state creep and plasticity, the integral (3) is independent from the path Γ when elastic strain rates are negligible throughout the body.

The reason why various creep condition do not affect the dependence of creep crack growth on the C^* parameter is that the C^* parameter itself already includes the effects of load level and temperature. That is, load level and temperature affect not only the creep crack growth rate but also the value of C^* parameter.

Once a steady-state distribution of stress and creep damage has been developed ahead of a crack tip, it is usually found that creep crack growth rate can be described by an expression of the form [9]:

$$\frac{da}{dt} = D \cdot C^{*\varphi} \quad (4)$$

where D and φ are material constants. Nikbin et al. [10] demonstrated that the power dependence of C^* varies only over the range 0.7-1 and the crack growth rate can be predicted by:

$$\frac{da}{dt} = \frac{3}{\epsilon_f^*} \cdot C^{*0.85} \quad (5)$$

Eq. 5 represents the NSW Model and is also included in the statement of the BS 7910 rule for the estimation of the creep crack propagation ratio in components operating at high temperature. In this model the extremes of plane stress and plane strain conditions are predicted taking into account the decrease of creep ductility under multiaxial stress conditions. The multiaxial ductility ϵ_f^* ranges between the uniaxial failure strain ϵ_f , for plain stress conditions, and 1/30 of the uniaxial failure strain for plain strain conditions [2, 9].

To verify the validity of the NSW model for the examined material, the C^* parameter may be determined by experimental test of CCG based upon the load line displacement rate, $\dot{\Delta}^c$,

$$C^* = \frac{P \dot{\Delta}^c}{B b} F \quad (6)$$

where P is the applied load, b the remaining ligament ahead the crack tip, B the net thickness, and F a factor dependent on crack length, specimen geometry and creep stress index n ; while in order to use the Eq. (5) for components, C^* must be determined from finite element analysis or, in line with the used defect assessment codes, from reference stress method.

In this paper a 12%Cr steel for turbine disk has been examined. CCG test on compact tension (CT) specimens according to the recommendations of ASTM-E1457 have been carried out in order to obtain K_{II} characterizing the creep crack initiation of the material (Eq. 2) and to validate the Eq. (4) for the correlation between creep crack growth and C^* parameter. For a turbine disk made of this examined 12%Cr steel, the 2CD diagram has been applied to study the occurrence of crack initiation on the component at the extreme stress level and temperature experienced in service and the correlation expressed by Eq. (5) has been used to compare the cracking behaviour of the turbine disk when C^* is numerically calculated by FEM analysis and when it is calculated by reference stress solution.

The usual load case for the turbine disk is a start/stop thermo-mechanical load including a hold time at high temperature, where this hold time load is high enough to cause time dependent effects such as creep deformation.

In order to support and validate the assessment procedures for these high temperature components, before their practical use, investigation about creep fatigue interaction phenomena are required, though the estimation of the creep crack initiation and growth rate represents the first essential step.

EXPERIMENTAL CCG TESTS

CCG test have been performed on CT specimens with width=25.4 mm and B=12.7 mm according to ASTM E1457 [11]. All the specimens were pre-cracked by fatigue at room temperature under the condition of a load ratio $R=0.005$. The lengths of the fatigue pre-cracks were about 1 mm. The tests were performed at constant load and at temperature between 450 °C and 510 °C with temperature control for all the specimens within 1 °C. Creep crack length was measured by DC electrical potential drop method. To convert electrical potential drop into crack length, the calibration equation derived in [12] for the ½ inch CT specimens was used.

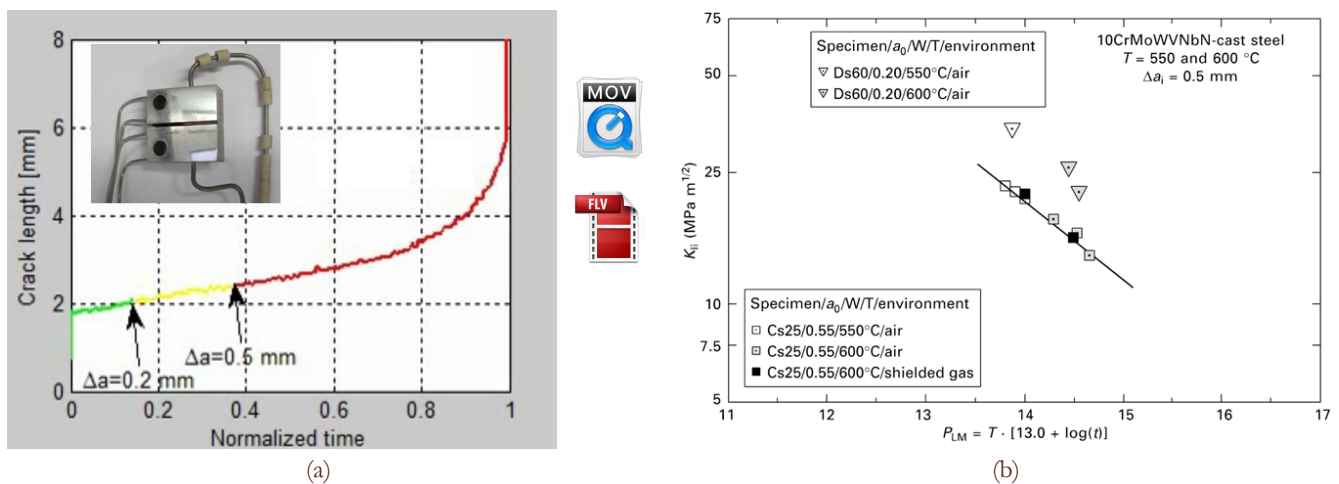


Figure 2: a) Crack length versus normalized time. The detail shows the specimen with the potential leads on the left and the current leads on the top and on the bottom surface of the specimen. b) Stress intensity factor at initiation of crack propagation (K_{Ii}) versus Larson Miller parameter [13].

Fig. 2a shows a typical example of crack length data collected during each crack growth test, from which the time of crack growth initiation (t_i) and the crack growth rate da/dt can be obtained. The time of crack growth initiation is defined as the time at which a significant crack growth, usually taken equal to 0.2 ± 0.5 mm, has been reached. From this graphs, and the corresponding load, also the value of the parameter K_{Ii} that characterizes the creep crack initiation of the material (see Eq. 2) can be obtained. An important feature of the parameter K_{Ii} is that data are not affected from the test temperature and converge on a linear trend, if plotted in semi logarithmic scale versus a Larson Miller parameter of the initiation time (t_i), as shown in Fig. 2b for literature data [13]. The trend of Fig. 2b has been fully confirmed by the results of the performed tests.

The experimental value of C^* to correlate with crack growth rate has been obtained from load line displacement rate following Eq. (6). It has been found that the dependence of crack growth rate da/dt on C^* parameter follows a near linear trend on log-log scale with a relative narrow scatter band. It indicates that crack growth rate correlates with C^* parameter according to Eq. (4), and that the C^* parameter is appropriate to describe the crack growth of this material. Moreover if the proper uniaxial creep ductility of the material ϵ_f is assumed equal to 1.55, as obtained from uniaxial creep tests at 500 °C and 550 °C, the creep growth rate predicted by the NSW model in the plain stress and plain strain conditions (Eq. 5) well represents the lower and the upper bound of the crack propagation ratio versus C^* for the investigated material.



CRACK GROWTH INITIATION

The Two Criteria Diagram has been applied for the calculation of the time t_i to initiate a crack extension, $\Delta a=0.5$ mm, of a circular/semicircular defect in the radial plane of a turbine disk. This value of the crack extension takes into account the time that is needed for creep damage to develop around the crack tip, but also the practical limitations of the crack detection equipment, for which the initiation crack growth on the component is difficult to be precisely determined.

Fig. 3 reports thermo-mechanical stress field on the cross section of turbine disk at the operating conditions, as obtained from finite element analysis. The highest values of thermo-mechanical stresses are experienced by the disk's hub in correspondence of the lowest temperatures.

For each node on the axisymmetric model three radius of the circular/semicircular defect have been considered, $R=0.5$ mm, 1 mm, 2 mm. According to the assessment of crack initiation by 2CD the different ratio, namely R_σ and R_k (Eq. 1 and 2), has been calculated as dependent on time. The nominal stress $\sigma_{n,pl}$ has been assumed equal to a reference stress based on a local collapse mechanism, and calculated as the mean value of the circumferential stress on a distance of 50 mm behind the crack tip. This approach is often recommended in defect assessment procedure [2] because results in a conservative determination of the reference stress. The loading parameter K_{Iid} has been calculated using the Shiratori weight functions [14]. The required material data $\sigma_R=\sigma_R(t_i)$ which represents the creep rupture strength of the material versus the rupture time, at the nodal temperature, and the parameter $K_{Ii} = K_{Ii}(t_i)$ characterizing the creep crack initiation of the material are obtained from the graph of Fig. 2b at a given nodal temperature.

For each nodal position and/or each crack radius the time t_i to initiate a crack extension, $\Delta a=0.5$ mm, is the value for which the point $(R_k(t_i), R_\sigma(t_i))$ crosses the border line crack/no crack of the 2CD.

Results have shown that the critical zone for the creep crack growth initiation is the hub area due to the high level of circumferential stresses. In this area, where also the smaller defect may be critical in the target time of 100000 hours of service, a detailed analysis of creep crack growth rate is necessary.

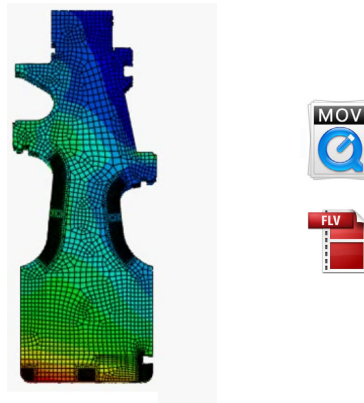


Figure 3: Thermo-mechanical stress field on turbine disk cross section.

CRACK GROWTH RATE ANALYSIS

The cracks propagation rate due to creep in hub of turbine disks has been related to the parameter C^* , in accordance with the NSW model (Eq. 5) for plain strain conditions, as validate by CCG experimental tests.

The calculation of the C^* parameter has been conducted numerically, by finite element analysis, but also with approximate methods based on the reference stress concept as proposed in the BS7910 Standard. Both procedures have been applied to the analysis of the creep growth rate for three semicircular cracks, $R=0.5$ mm, 1 mm, 2 mm, in two different superficial positions of the turbine disk hub, in order to compare and discuss the results.

Numerical procedure

In this study the procedure summarized in the flowchart of Fig. 4a has been used for the FEM calculation of the C^* parameter, related to semi-circular defects on the hub of the turbine disk. According to the definition, the C^* contour integral (Eq. 3) has been calculated as asymptotic value of the time dependent $C(t)$ integral versus time. All numerical

analysis and contour integrals calculation have been conducted with code Abaqus version 6.11. The size of the mesh refinement, required for the calculation of the C^* fracture mechanics parameter, suggests the use of the submodelling technique.

The starting point of the procedure is a steady state thermal analysis on an axisymmetric model of the disk turbine built with reduced integration 8 node elements. The surface temperatures and the associated heat transfer coefficients have been assumed as boundary conditions, for the calculation of the temperature field on the cross section of the turbine disk. The second step of the procedure is a thermo-mechanical analysis followed by a visco-elastic analysis, carried out on a three-dimensional model of a sector of the disk (Fig. 4b). Reduced integration 20 node elements have been used for the solid model. According the submodelling technique, this model represents the global model of the turbine disk and is crack free. With the global thermo-mechanical model, at first the thermal stresses associated to the nodal temperature distribution have been calculated. Then the mechanical stresses, due to the applied mechanical load with the addition of the centrifugal speed, have been calculated, by means a static analysis assuming the elasto-plastic behaviour of the material, and superimposed to the thermal stress. The obtained nominal distribution of thermo-mechanical stresses on the turbine disk represents the initial condition for the subsequent visco-elastic analysis. The visco-elastic analysis, calculates the transient of the stress relaxation on the global model for a total time of 100000 h, assuming an appropriate Norton law for the material. For computational efficiency, a combined explicit and implicit integration scheme was used for creep calculation.

The FEM calculation of the C^* parameter has been performed for three semicircular cracks, $R=0.5$ mm, 1 mm, 2 mm, both in the positions 1 and 2 of the turbine disk hub (Fig. 4b). As reported in the same figure, for each crack a submodel has been prepared using reduced integration 20 node elements and with a focused mesh along the crack front. Moreover eight contours for the calculation of the $C(t)$ integral, have been defined for each node of the crack front.

The behaviour of the material is defined as in the global model of the turbine disk. The transient of the stress relaxation along the crack front has been calculated for a total time of 100000 h, with a visco-elastic analysis as in the global model. At each time of the transient, the nodal displacement on the surface delimiting the submodel, with respect to the global model, have been set equal to the ones in the global model at the same time. The results, in terms of relaxation of von Mises stresses, for the crack with radius equal to 1 mm in the Position 1, are shown in Fig. 5. After 100000 hours of FE simulation stress can be considered constant and consequently a stabilized C^* value can be determined.

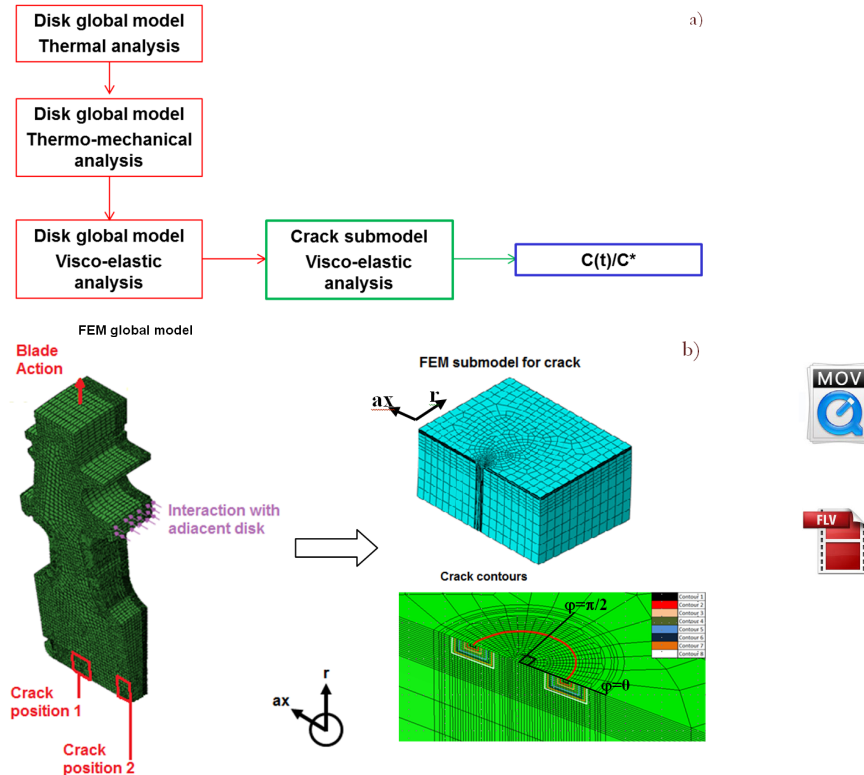


Figure 4: a) Procedure for numerical calculation of the C^* parameter related to semi-circular defects of a turbine disk. b) Tridimensional model of a sector of the turbine disk (the sector covers an angle equal to 10°), submodel of the crack and eight contours for the $C(t)$ calculation at each node of the crack front.



The $C(t)$ integral along the crack front has been extracted from the FE results as function of time t . At each node of the crack front, under transient conditions it exhibits significant path-dependence, while as the steady state creep condition is reached, it results almost path-independent and trending to the asymptotic value C^* . Fig. 6 shows the eighth contour values of the integral $C(t)$ at $\varphi=\pi/2$ of the crack front during the 100000 h viscoelastic analysis. The crack is in Position 1 of Fig. 4b and the results are reported for the three values of the radius $R=0.5$ mm, $R=1$ mm and $R=2$ mm. The $C(t)$ value in correspondence of 100000 h was taken as the parameter C^* to correlate the stable crack growth rate at high temperature on the turbine disk. The calculated values of the C^* parameter are summarized in Tab. 1. In the same table is reported the estimated steady state crack growth rate according to the NSW model for plain strain conditions (Eq. 5) and based on the finite element calculation of the C^* parameter.

Reference Stress Solution

The reference stress solution is, also, used to calculate the creep propagation rate for the same series of defects studied by means of a FEM analysis. With this approach, in line with the one used in the defect assessment codes [2], a guide to the creep propagation ratio is expressed approximately as:

$$\frac{da}{dt} = 0.014 \left(\frac{K^2}{\sigma_{ref} t_{ref}} \right)^{0.85} \tag{7}$$

where t_{ref} is the rupture time in the creep test at the proper σ_{ref} evaluated for the component, and K is the stress intensity factor:

$$K = 0.7 \sigma_{\theta} \sqrt{\pi \cdot R} \tag{8}$$

where σ_{θ} is the circumferential stress on the component and R is the radius of the semicircular crack.

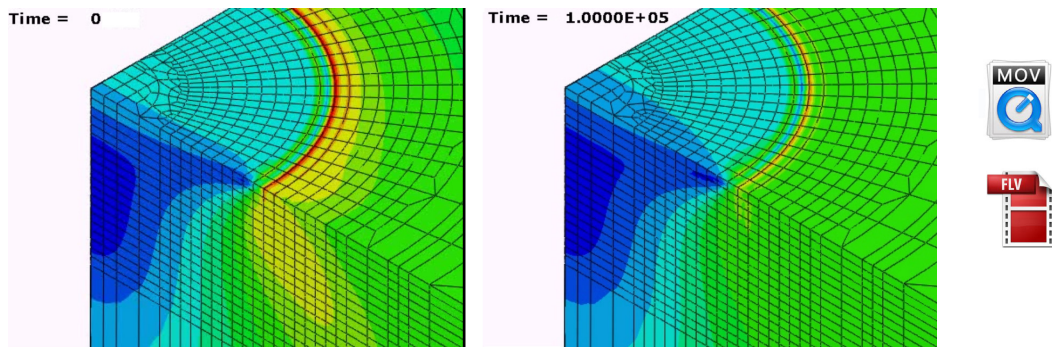


Figure 5: Relaxation of von Mises stresses for the crack with radius equal to 1 mm in the Position 1 of Fig. 4b. Only half of the crack is shown at 0 and 100000 hours of simulation.

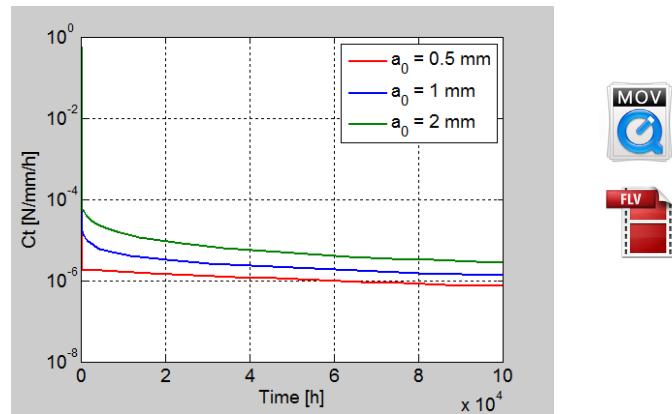


Figure 6: Eighth contour value of the $C(t)$ integral at $\varphi=\pi/2$ for the crack is in the Position 1 of Fig. 4b.



	R [mm]	C* [N/mm/n]	(da/dt) [mm/h]
Position 1	0.5	7.25E-07	9.54E-07
	1	1.35E-06	1.67E-06
	2	2.76E-06	3.07E-06
Position 2	0.5	8.85E-07	1.14E-06
	1	1.62E-6	1.95E-06
	2	3.15E-6	3.44E-06

Table 1: C* parameter at $\varphi=\pi/2$ for the crack in the Position 1 of Fig. 4b and creep crack growth rate.

In this paper σ_{ref} , as previously said, has been calculated, according to a conservative local collapse mechanism, as the mean value of the circumferential stress on a distance of 50 mm behind the crack tip. The rupture time t_{ref} has been obtained from the Larson Miller rupture curve of the material. Tab. 2 reports the estimated steady state crack growth rate according to the approximated approach based on the reference stress solution (Eq. 7). As the reference stress assumes the same value for both position of the crack, the predicted crack growth rate is the same for the two examined positions. Because the scatter of the rupture data of the material greatly affects the creep crack growth rate estimation, the used defect assessment code [2] suggests the use of safety factor between 1 and 10 on the average value of the rupture time. In Tab. 2 the predicted creep crack growth rate is reported for a safety factor equal to 1, 5, and 10.

A comparison between the creep crack growth rate, based on detailed finite element calculation of the fracture mechanics C* parameter and the estimated creep crack growth rate based on the reference stress solution, allows us to conclude that the approximate solution may not be conservative if an adequate safety factor on the rupture time is not introduced.

	R [mm]	t_{ROTT} [h]	(da/dN) [mm/h]	$t_{ROTT}/5$ [h]	(da/dN) [mm/h]	$t_{ROTT}/10$ [h]	(da/dN) [mm/h]
Position 1 and 2	0.5	1.1e+8	4.9e-7	2.2e+7	1.9e-6	1.1e+7	3.5e-6
	1	1.1e+8	8.9e-7	2.2e+7	3.5e-6	1.1e+7	6.3e-6
	2	1.1e+8	1.6e-6	2.2e+7	6.3e-6	1.1e+7	1.1e-5

Table 2: Estimated steady state crack growth rate according to the approximated approach based on the reference stress solution.

CONCLUSIONS

In this paper a 12%Cr steel for turbine disk has been examined. CCG tests on compact tension (CT) specimens according to the recommendations of ASTM-E1457 have been carried out, in order to obtain parameters characterizing the creep crack initiation of the material, and to evaluate the proper fracture mechanics parameter which defines the creep crack growth behaviour of the material. The results have been applied to study the occurrence of crack initiation on a turbine disk made of the examined material at the extreme stress level and temperature experienced in service, and to validate the use of the C* integral in correlating creep growth rate on the component, both when C* is numerically calculated through FEM analysis and reference stress solution.

It has been shown that predictions of creep crack growth can be very sensitive to the collapse mechanism assumed to determine the reference stress as well as to the material creep properties chosen. With recent advances in finite element (FE) methods, more complex approaches can be applied in the study of CCG, which may provide more accurate predictions than relatively simple analytical solutions.

ACKNOWLEDGMENTS

The work is part of the activities within the research project “Rotor disks life evaluation” between the Department of Mechanical Engineering at Politecnico di Milano and Ansaldo Energia. Prof. Stefano Beretta and Ing. Emanuela Cavalleri are thanked for guidance and useful discussions.



REFERENCES

- [1] Ainsworth, R. A., Hooton, D. G., R6 and R5 procedures: the way forward, *Int. Journal of Pressure Vessels and Piping*, 85 (2008) 175-182.
- [2] British Standard. BS 7910: Guide on Methods for Assessing the Acceptability of Flaws in Metallic Structures, BSI, (2005).
- [3] Kocak, M., Webster, S., Janosch, J.J., Ainsworth, R.A., Koers, R., FITNET Fitness-for-Service (FFS)- procedure, GKSS Research Centre, Germany, ISBN 978-3-940923-00-4, I (2008).
- [4] Mueller, F., Scholz, A., Berger, C., Comparison of different approaches for estimation of creep crack initiation, *Engineering Failure analysis*, 14 (2007) 1574-1585.
- [5] Ewald, J., Sheng, S., Klenk, A., Schellenberg, G., Engineering guide to assessment of creep crack initiation on components by two criteria diagram, *International journal of pressure vessels and piping*, 78 (2001) 937-949.
- [6] Granacher, J., Klenk, A., Tramer, M., Schellenberg, G., Mueller, F., Ewald, J., Creep fatigue crack behaviour of two power plant steels, *International journal of pressure vessels and piping*, 78 (2001) 909-920.
- [7] Zhang, S., Chai, G., Lu, Y., Study on the governing parameter of creep crack growth for 20g steel, *Journal of Pressure Equipment and Systems*, 4 (2006) 116-119.
- [8] Ainsworth, A., Lei, Y., Creep crack growth assessment methods, *Anales de mecanica de la fractura*, 26(1) (2009).
- [9] Ha, J., Tabuchi, M., Hongo, H., Toshimitsu, A. Jr, Fuji, A., Creep crack Growth properties for 12CrWCoB rotor steel using circular notched specimens, *International Journal of Pressure Vessels and Piping*, 81 (2004) 401-407.
- [10] Maleki, S., Zhang, Y., Nikbin, K., Prediction of Creep Crack growth properties of P91 parent and welded steel using remaining failure strain criteria, *Engineering fracture Mechanics*, 77 (2010) 3035-3042.
- [11] ASTM E 1457-07: Standard Test Method for Measurement of Creep Crack Growth Rates in Metals, (2007).
- [12] Belloni, G., Gariboldi, E., Lo Conte, A., Tono M., Speranzoso, P., On the experimental calibration of potential drop system for crack length of compact tension specimen measurements, *Journal of Testing and Evaluation*, 30 (2002) 461-469
- [13] Mueller, F., Scholz, A., Berger, C., Klenk, A., Maile K., Roos, E., Crack Behaviour of 10Cr-steels under Creep and Creep-Fatigue Conditions, In: ECCC Creep Conference, London (UK), (2005) 685-699.
- [14] Shiratori, M., Miyoshi, T., Tanikawa, K., Analysis of Stress Intensity Factors for surface cracks subjected to arbitrarily distributed surface stresses. In: Murakami Y., editor, *Stress Intensity Factors Handbook*, chapter Weighting function for a semi-elliptical surface crack in a plate under basic mode of stress distribution, Pergamon Press, Oxford, (1987) 725-727.